This article has been accepted for publication in a future issue of this journal, but has not been fully edited. Content may change prior to final publication. Citation information: DOI 10.1109/TIE.2021.3094488, IEEE Transactions on Industrial Electronics

Experimentally Validated Extended Kalman Filter Approach for Geomagnetically Induced Currents Measurement

Behzad Behdani, Mohsen Tajdinian, Mehdi Allahbakhshi, *Member, IEEE*, Marjan Popov, *Senior Member, IEEE*, Miadreza Shafie-khah, *Senior Member, IEEE*, and João P. S. Catalão, *Senior Member, IEEE*

***Abstract*—Geomagnetically induced currents (GICs) are referred to as the quasi-DC current flows in power networks, driven by complex space weather-related phenomena. Such currents are a potential threat to the power delivery capability of electrical grids. To mitigate the detrimental impacts of GICs on critical infrastructures, the GICs should be monitored in power systems. Being inherently DC from the power frequency point of view, the components of GICs are, however, challenging and costly to monitor in AC power grids. This paper puts forward a novel methodology for the real-time estimation of GICs in power transformers. Such aim is attained by means of an extended Kalman filter (EKF)-based approach, mounted on the nonlinear state-space model of the transformer, whose parameters can be derived from standard tests. The proposed EKF-based algorithm employs the available measurements for the transformer differential protection. The proposed approach, relying on the differential current, can properly deal with the external sources of interference like harmonic excitation and loading. The EKF-based estimator presented is validated by simulation and experimental data. The results verify the ability of the proposed approach to robustly estimate the GIC level during various operating conditions.**

***Index Terms*—Extended Kalman filter, geomagnetically induced current, Power Transformer.**

NOMENCLATURE

i_{ac}	AC component of differential current
R_b	Bypass resistor in the test setup
R_c	Core loss equivalent resistance
L_m	Core magnetization equivalent inductance
$\boldsymbol{P}$	Covariance matrix of estimation error
φ_{DC} φ_{AC}	DC and AC core flux component magnitudes
U_{dc}	DC voltage simulating GIC effect
I_0, I_1, I_2, I_3,	DC, 1st, 2nd, and 3rd harmonic magnitudes
I_{dc}	Effective GIC
Abs. Error	Estimation error absolute value
Avg. Error	Estimation error absolute value average
Error%	Estimation error percentage
Avg. Error%	Estimation error percentage average
$\hat{\boldsymbol{x}}$	Estimation of the state vector
$\hat{\lambda_1}$, $\hat{\lambda_2}$, $\hat{\lambda_m}$, $\hat{I}_{dc}$	Estimation of λ_1, λ_2, λ_m, I_{dc}
j	Estimation sample number j
n	Estimation samples total number
i_c	Excitation current's core loss component
i_m	Excitation current's magnetizing component
λ_m	Flux linkage of magnetization inductance
λ_{L1}	Flux linkage of primary winding inductance
$\lambda_{L'2}$	Flux linkage of secondary winding inductance
$\bar{E}$	Geoelectric field (GEF) due to GMDs
$d\bar{l}$	Incremental path segment of transmission line
$\boldsymbol{P_0}$	Initial value for $\boldsymbol{P}$
$\boldsymbol{x}_0$	Initial value for the state vector
$\boldsymbol{K}$	Kalman filter gain matrix
$\widetilde{\boldsymbol{Q}}$	Linearized equivalent of $\boldsymbol{Q}$
$\widetilde{\boldsymbol{R}}$	Linearized equivalent of $\boldsymbol{R}$
R'_l	Load equivalent resistance
H	Magnetic field strength
B	Magnetic flux density
$\boldsymbol{y}$	Measurement vector
$\boldsymbol{R}$	Noise covariance matrix of measurement
$\boldsymbol{Q}$	Noise covariance matrix of process
Ω_n	Nominal rotational frequency of the system
$\boldsymbol{\omega}_0$ and $\boldsymbol{v}_0$	Nominal values of $\boldsymbol{\omega}$ and $\boldsymbol{v}$
$\boldsymbol{h}$	Nonlinear measurement matrix function
$\boldsymbol{f}$	Nonlinear state transition matrix function
E_N and E_E	Northward and Eastward GEF components
L_N and L_E	Northward and Eastward line lengths
$\boldsymbol{A}$, $\boldsymbol{N}$, $\boldsymbol{C}$, $\boldsymbol{M}$	Partial derivative matrices
i_1 and i'_2	Primary and Secondary side currents
e_1 and e'_2	Primary and Secondary side voltages
L_1 and L'_2	Primary and Secondary winding inductances
R_1 and R'_2	Primary and Secondary winding resistances
$\boldsymbol{\omega}$ and $\boldsymbol{v}$	Process and measurement noise matrices
$\boldsymbol{x}$	State vector
S_1 and S_2	Switches in the test setup
$\boldsymbol{F}$	System matrix
$\boldsymbol{u}$	System's control input vector
CT_1 and CT_2	Test current transformers
T_1 and T_2	Test transformers
t	Time
R_n	Transformer neutral connection resistance
r	Transmission line route
a_1	λ_m- i_m characteristic linear part factor
a_γ	λ_m- i_m characteristic nonlinear part factor
γ	λ_m- i_m characteristic odd order of polynomial

B. Behdani, M. Tajdinian, and M. Allahbakhsh are with the School of Electrical and Computer Engineering, Shiraz University, Shiraz, Iran (e-mails: b.behdani@shirazu.ac.ir; tajdinian.m@shirazu.ac.ir; allahbakhshi@shirazu.ac.ir).

M. Popov is with the Faculty of Electrical Engineering, Mathematics and Computer Science, Delft University of Technology, 2628 Delft, The Netherlands (e-mail: m.popov@tudelft.nl).

M. Shafie-khah is with School of Technology and Innovations, University of Vaasa, Vaasa 65200, Finland (e-mail: mshafiek@univaasa.fi).

J.P.S. Catalão is with the Faculty of Engineering of the University of Porto (FEUP) and INESC TEC, Porto 4200-465, Portugal (e-mail: catalao@fe.up.pt).

I. INTRODUCTION

OVER the past years, there has been an increasing rise of attention toward the impacts of system disturbances introduced by complex space weather-driven phenomena. These phenomena are originated from violent eruptions of high-energy charged particles from the Sun's atmosphere towards the Earth. Upon arrival, the winds of solar particles cause geomagnetic disturbances (GMDs), resulting in the slow temporal fluctuation of naturally flowing currents in the ionosphere, known as electrojets [1].

0278-0046 (c) 2021 IEEE. Personal use is permitted, but republication/redistribution requires IEEE permission. See http://www.ieee.org/publications_standards/publications/rights/index.html for more information.
Authorized licensed use limited to: b-on: UNIVERSIDADE DO PORTO. Downloaded on July 08,2021 at 16:36:40 UTC from IEEE Xplore. Restrictions apply.

This article has been accepted for publication in a future issue of this journal, but has not been fully edited. Content may change prior to final publication. Citation information: DOI 10.1109/TIE.2021.3094488, IEEE Transactions on Industrial Electronics

The time-varying electrojets, in return, induce quasi-DC geoelectric fields (GEFs) over the man-made infrastructure at the Earth's surface, such as power networks. Accordingly, GEF-induced potentials are integrated along transmission conductors, driving the quasi-DC GICs through a closed path comprising the transmission lines, grounded-star transformers, and the conductive surface of Earth [2]. Fig. 1 illustrates the physical mechanism of geomagnetic induction, as described.

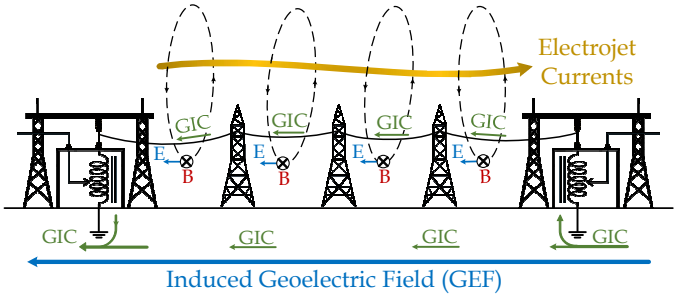

Fig. 1. The physical mechanism of geomagnetic induction.

The primary effect of the GICs on AC power systems is through the half-cycle saturation of power transformers. This phenomenon leads to elevated harmonic generation in the transformer magnetizing current [3], which in turn, severely affects the power system continuity of operation through relay maloperation [4], ferroresonance [5], equipment overheating [7], elevated reactive power demand [8], and eventually large-scale blackout, similar to the Hydro-Quebec power system's blackout on March 13-14, 1989 [9].

The necessity to develop an insight towards the flow of GICs in the power system is manifested by the need to provide adequate mitigatory solutions [6]-[8] against the impacts of GICs as they rise up to threatening levels. However, the GICs appearing as DCs from the power frequency point of view, are costly and challenging to access. One GIC estimation technique is through power system simulation approaches, e.g., by using power flow techniques to simulate the flow of GICs [10], employing the magnetic field measurements in the power grid area [11], and a model for the Earth's conductivity, using techniques such as [12].

There are several drawbacks to such techniques; the considerations simplifying the complexities associated with measured magnetic fields, the Earth's conductivity, and power network simulations pile up cumulatively, resulting in a high order of uncertainty and error. Moreover, the performances of the equipment under GICs are barely reflected by having determined the GICs circulating in the network [13].

Conventional measurements in AC systems via voltage transformers (VTs) and current transformers (CTs) are unable to measure DC components. However, such measurements can be carried out on selected transformers through Hall-effect sensors installed on their neutral conductor [14].

Neutral current monitoring is also associated with plenty of defects; as only the selected neutrals are monitored, the installation of GIC monitors on every transformer would be costly. Furthermore, the neutral current does not reflect the level of half-cycle saturation in the case of autotransformers.

CTs have been employed by [15] to indirectly measure the DC current flow in a conductor, based on the measured even harmonics; however, the GIC monitoring can be affected by the interferences from the harmonics with external sources such as nonlinear loads, and also the thermal noise from transformer overheating due to saturation. The effect of external harmonics has been canceled by the technique in [16], which estimates the GICs flowing through transformer windings by measuring the 2nd harmonic component of the magnetizing current.

Nevertheless, it is shown by [17] that the magnetizing current harmonics vary as the level of GICs increases. As the harmonic-based measurement techniques do not consider the complex behavior of the GIC-generated harmonic contents, they are ineffective under severe half-cycle saturation conditions where accurate measurement is even more crucial. By measuring the transformer reactive power absorption, references [13] and [18] proposed a technique for the estimation of GICs in transformers. The calculations for this method are, however, conducted considering only the fundamental frequency component, which is (owing to high levels of harmonics in the presence of GICs) negligent. In addition, this method also fails to consider the aforementioned complex behaviors under severe GICs.

A recent study by [19] utilized a machine learning approach to detect GICs in power grids. This approach, apart from the conventional drawbacks of machine learning, e.g., requiring huge training datasets, also defects in GIC monitoring as it solely aims at detecting GICs in power systems.

The availability of accurate GIC measurement in real-time, being crucial for operational decision-making to preserve the power delivery continuity, is what the existing monitoring tools and mechanisms fail in. Hence, in this paper, a new technique is proposed for the real-time estimation of GICs in transformer windings by measuring the AC component of the transformer magnetizing current, readily available from the differential protection scheme. The proposed technique is sought by the employment of an extended Kalman filter (EKF), mounted on the nonlinear state-space model of the transformer. The model parameters required by EKF are either provided by manufacturers or can be easily obtained via standard transformer test data [20]-[22].

The contributions of the proposed method are as follows:

- Compared to the present techniques [14], which require GIC monitoring equipment, the proposed method can be swiftly employed using the existing AC measurements for the transformer differential protection scheme.
- Unlike previous GIC metering methods, the proposed EKF-based approach accounts for wide GIC ranges with good accuracy as it properly deals with nonlinear complexities.
- The presented method is resistive to external interferences and demonstrates robustness against measurement and process noise under various operation conditions.

The rest of the paper is organized as follows: The process through which the GICs impact power systems, motivating the necessity of a real-time GIC estimator, is surveyed alongside the basics for extended Kalman filtering in Section II. In Section III, the proposed method is outlined by first deriving the nonlinear state-space representation of the estimation model and then formulating the problem for the EKF estimator. The feasibility and accuracy of the proposed

0278-0046 (c) 2021 IEEE. Personal use is permitted, but republication/redistribution requires IEEE permission. See http://www.ieee.org/publications_standards/publications/rights/index.html for more information.
Authorized licensed use limited to: b-on: UNIVERSIDADE DO PORTO. Downloaded on July 08,2021 at 16:36:40 UTC from IEEE Xplore. Restrictions apply.

This article has been accepted for publication in a future issue of this journal, but has not been fully edited. Content may change prior to final publication. Citation information: DOI 10.1109/TIE.2021.3094488, IEEE Transactions on Industrial Electronics

approach are verified by simulation and experimental results presented in Section IV. Conclusions are stated in Section V.

II. Principles and Basics

In order for presenting a systematic approach towards the proposed EKF-based GIC estimator, the basic principles on which this study is established are surveyed in the following sub-sections.

A. Transformer Unidirectional Saturation due to GICs

The most realistic practice to characterize GICs is through series DC voltage source U_{dc}, representing the potentials induced over the transmission conductor as a result of the GMD-induced GEF variations [23], found by the integration of geoelectric field $\bar{E}$ over the incremental path segment $d\bar{l}$ of transmission line route r, as:

$$U_{dc} = \int_r \bar{E} \,.\, d\bar{l} \,. \tag{1}$$

Assuming a uniform GEF, the DC voltage induced along the transmission conductor is obtained by:

$$U_{dc} = E_N L_N + E_E L_E \,. \tag{2}$$

The induced voltages drive GICs in transformer windings, establishing a DC flux in the core and forcing the transformer into nonlinear operation. As implied by the recommendations for low-frequency transients [24], the nonlinearity of the transformer iron core can be modeled by a two-term odd-order polynomial relationship between i_m and λ_m as:

$$i_m = a_1 \lambda_m + a_\gamma \lambda_m^\gamma \,. \tag{3}$$

Considering the transformer core flux to be comprised of a DC, with a sinusoidal AC part, the following can be imagined:

$$\lambda_m = \varphi_{DC} + \varphi_{AC} \cos(\Omega_n t) \,. \tag{4}$$

Substituting (4) in (3), and considering $\gamma=3$ [5], i_m becomes:

$$i_m = I_0 + I_1 \cos(\Omega_n t) + I_2 \cos(2\Omega_n t) + I_3 \cos(3\Omega_n t) \,. \tag{5}$$

It is evidently deduced that the existence of DC flux offset in the transformer's core results in the 2nd harmonic generation in its magnetizing current, indicating its core's saturation. Accordingly, the linear considerations are no longer valid, and the transformer parameters express complex behaviors in response to different GIC levels [17], [19]. Such behaviors, add yet another level of difficulty to the GIC measurement issue, calling for an approach robust to nonlinear complexities.

B. Extended Kalman filter

The Kalman filter is an optimal estimation tool, establishing the foundation for a wide variety of algorithms, each developed in consideration for a certain set of problems. The standard Kalman filter only applies to linear systems. However, the basic idea of Kalman filtering can be extended by the linearization of nonlinear systems around the state trajectory estimated by the Kalman filter itself [25].

The extended Kalman filter (EKF) robustly performs under highly distorted conditions and excellently tackles model uncertainty and measurement noise, providing accurate estimations. One of the most practical properties of Kalman filtering is its capability to estimate the system states, unable to be measured directly.

Kalman filtering is employed in power systems for dynamic state estimation in a variety of applications [26]-[28]. In order to achieve a unified understanding, the theoretical basis of the EKF algorithm is briefed in the following.

A nonlinear system in its generic form can be described as:

$$\begin{aligned} \dot{\boldsymbol{x}} &= \boldsymbol{f}(\boldsymbol{x}, \boldsymbol{u}, \boldsymbol{\omega}, t) \\ \boldsymbol{y} &= \boldsymbol{h}(\boldsymbol{x}, \boldsymbol{v}, t) \\ \boldsymbol{\omega} &\sim (0, \boldsymbol{Q}) \\ \boldsymbol{v} &\sim (0, \boldsymbol{R}) \end{aligned} \tag{6}$$

where the system is assumed to contain zero-mean multivariate Gaussian noises $\boldsymbol{\omega}$ and $\boldsymbol{v}$ with covariance matrices $\boldsymbol{Q}$ and $\boldsymbol{R}$, corresponding to the process and measurement.

The EKF methodology is comprised of two consecutive steps for prediction and update. Initially, the *a priori* estimation of system states is carried out from the nonlinear system model. Having considered the process to be of white uncorrelated noise, *a priori* estimate of the error covariance is obtained. Thereafter, the partial derivative matrices $\boldsymbol{A} = \frac{\partial \boldsymbol{f}}{\partial \boldsymbol{x}}\Big|_{\hat{\boldsymbol{x}}}$, $\boldsymbol{N} = \frac{\partial \boldsymbol{f}}{\partial \boldsymbol{\omega}}\Big|_{\hat{\boldsymbol{x}}}$, $\boldsymbol{C} = \frac{\partial \boldsymbol{h}}{\partial \boldsymbol{x}}\Big|_{\hat{\boldsymbol{x}}}$, and $\boldsymbol{M} = \frac{\partial \boldsymbol{h}}{\partial \boldsymbol{v}}\Big|_{\hat{\boldsymbol{x}}}$ are calculated and employed together with actual measurements $\boldsymbol{y}$ for calculation of the Kalman gain, which is used to update the system states by the *a posteriori* estimate. Finally, assuming the measurements contain white uncorrelated noise, *a posteriori* estimate of the error covariance $\boldsymbol{P}$ is attained, which is used for the prediction stage within the subsequent sampling instant. The speed and accuracy of EKF-based estimators for nonlinear systems are ensured by such recursive methodology.

As described previously, the GIC flow through transformer windings results in half-cycle core saturation, i.e., nonlinear operation. Although the transformer magnetizing current is monitored via the conventionally employed differential protection scheme, its DC component is simply neglected by CTs. However, EKF makes it possible for a nonlinear system's state to be estimated when its direct measurement is not possible. Based on such a principle, the proposed technique aims at utilizing an EKF to estimate GICs in transformers via existing differential protection measurements.

III. Proposed Approach

A. State-Space Representation of the Estimation Model

To implement an EKF-based estimator, a state-space model of the problem is required. In this section, the nonlinear equations describing the behavior of such a model are derived.

The estimation model is according to the circuit in Fig. 2. Given the argument made in the previous section, that the GMDs impose DC voltages on transmission conductors, the effect of GICs is modeled by the DC voltage source U_{dc}.

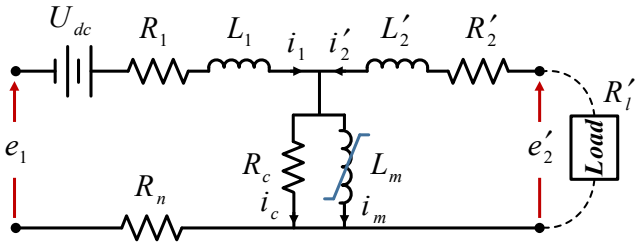

Fig. 2. The estimation model representation.

0278-0046 (c) 2021 IEEE. Personal use is permitted, but republication/redistribution requires IEEE permission. See http://www.ieee.org/publications_standards/publications/rights/index.html for more information.
Authorized licensed use limited to: b-on: UNIVERSIDADE DO PORTO. Downloaded on July 08,2021 at 16:36:40 UTC from IEEE Xplore. Restrictions apply.

This article has been accepted for publication in a future issue of this journal, but has not been fully edited. Content may change prior to final publication. Citation information: DOI 10.1109/TIE.2021.3094488, IEEE Transactions on Industrial Electronics

Employing KCL in the center node and KVL in the input and output loops of the circuit in Fig. 2, the following is obtained:

$$i_1 + i'_2 = i_m + i_c \,, \tag{7}$$

$$e_1 + U_{dc} = (R_1 + R_n)i_1 + \frac{d\lambda_1}{dt}, \tag{8}$$

$$e'_2 = R'_2 i'_2 + \frac{d\lambda_2}{dt}. \tag{9}$$

where $\lambda_1=\lambda_{L1}+\lambda_m$, and $\lambda_2=\lambda_{L'2}+\lambda_m$. Yielding the linearity of L_1 and L'_2 by $\lambda_{L1}=L_1 i_1$ and $\lambda_{L'2}= L'_2\, i'_2$; currents i_1 and i'_2 are:

$$i_1 = \frac{\lambda_1 - \lambda_m}{L_1} \,, \tag{10}$$

$$i'_2 = \frac{\lambda_2 - \lambda_m}{L'_2}. \tag{11}$$

Also, the center loop KVL of the equivalent circuit yields:

$$R_c i_c = \frac{d\lambda_m}{dt} \,. \tag{12}$$

Substituting (10) in (8), and considering the DC component of magnetizing current (the effective GIC) driven by U_{dc} as $I_{dc}=U_{dc}/(R_1+R_n)$, the first state-space equation is given by:

$$\frac{d\lambda_1}{dt} = -\frac{R_1 + R_n}{L_1}\lambda_1 + \frac{R_1 + R_n}{L_1}\lambda_m + (R_1 + R_n)I_{dc} + e_1 \,. \tag{13}$$

Substituting (11) in (9), and considering $e'_2=-R'_l i'_2$, the second state-space equation is obtained as:

$$\frac{d\lambda_2}{dt} = -\frac{R'_2 + R'_l}{L'_2}\lambda_2 + \frac{R'_2 + R'_l}{L'_2}\lambda_m \,. \tag{14}$$

Incorporating the relations (10)-(12) together with (3) and (7), the third state-space equation is derived as:

$$\begin{aligned}\frac{d\lambda_m}{dt} &= \frac{R_c}{L_1}\lambda_1 + \frac{R_c}{L'_2}\lambda_2 \\ &-R_c\left[\left(\frac{L_1 + L'_2}{L_1 L'_2}\right) + a_1 + a_\gamma \lambda_m^{\gamma-1}\right]\lambda_m \,.\end{aligned} \tag{15}$$

Finally, considering the DC behavior of GICs, the fourth state-space equation is given by:

$$\frac{dI_{dc}}{dt} = 0 \,. \tag{16}$$

In addition, the nonlinear model's output is provided by CT measurements for the transformer differential current as:

$$\begin{aligned}i_{ac} &= i_1 + i'_2 - I_{dc} \\ &= \frac{1}{L_1}\lambda_1 + \frac{1}{L'_2}\lambda_2 - \left(\frac{L_1 + L'_2}{L_1 L'_2}\right)\lambda_m - I_{dc} \,.\end{aligned} \tag{17}$$

Equations (13)-(17) form the state-space description of the transformer under study by state variables selected as follows:

$$\boldsymbol{x} = [\lambda_1 \quad \lambda_2 \quad \lambda_m \quad I_{dc}]^T \,. \tag{18}$$

B. Formulation of the EKF-based GIC Estimator

To begin with the implementation of the proposed EKF-based estimator, first, the nonlinear system should be represented by its state-space model, as in the form of (6).

According to the derived state-space representation of the estimation model in the previous sub-section, $\boldsymbol{x}^{4\times 1}$ is the state vector given in (18), $\boldsymbol{u}=e_1$ is the transformer input voltage, $\boldsymbol{y}=i_{ac}$ is the measured transformer differential current. It should be noted that matrices $\boldsymbol{Q}$ and $\boldsymbol{R}$ are defined based on modeling and measurement uncertainties, respectively [25].

In this study, $\boldsymbol{R}$ is obtained by processing the measurements while holding the system output constant. To such an aim, the noise effect is extracted from the data by removing its mean and calculating the covariance from the remained data portion.

On the other hand, $\boldsymbol{Q}$, reflecting the unmodelled dynamics and parameter uncertainties, is not rather straightforward. Therefore, in this paper, $\boldsymbol{Q}$ is obtained by performing a sensitivity analysis to achieve the best results.

Based on the considerations above, by substituting the derived state-space equations (13)-(17) in the general form (6) and considering additive noise, the equation system is defined as:

$$\begin{bmatrix}\dot{\lambda}_1 \\ \dot{\lambda}_2 \\ \dot{\lambda}_m \\ \dot{I}_{dc}\end{bmatrix} = \boldsymbol{F}^{4\times 4} \times \begin{bmatrix}\lambda_1 \\ \lambda_2 \\ \lambda_m \\ I_{dc}\end{bmatrix} + \begin{bmatrix}1 \\ 0 \\ 0 \\ 0\end{bmatrix} e_1 + \begin{bmatrix}\boldsymbol{\omega}(1) \\ \boldsymbol{\omega}(2) \\ \boldsymbol{\omega}(3) \\ \boldsymbol{\omega}(4)\end{bmatrix}$$

; $\mathbf{F}^{4\times 4}$

$$= \begin{bmatrix} -\frac{R_1 + R_n}{L_1} & 0 & \frac{R_1 + R_n}{L_1} & (R_1 + R_n) \\ 0 & -\frac{R'_2 + R'_l}{L'_2} & \frac{R'_2 + R'_l}{L'_2} & 0 \\ \frac{R_c}{L_1} & \frac{R_c}{L'_2} & -R_c\left(\left(\frac{L_1 + L'_2}{L_1 L'_2}\right) + a_1 + a_\gamma \lambda_m^{\gamma-1}\right) & 0 \\ 0 & 0 & 0 & 0 \end{bmatrix} \tag{19}$$

It is worth noting that the proposed method is based on the transformer's measured differential current, denoted by $\boldsymbol{y}=i_{ac}$ as in (17). According to the relationships in (19), the partial derivative matrices $\boldsymbol{A}$, $\boldsymbol{N}$, $\boldsymbol{C}$, and $\boldsymbol{M}$ are derived as in (20)-(23). The estimation process of the proposed method, as explained in the previous section, is illustrated by the flowchart in Fig. 3.

$$\boldsymbol{A} = \left.\frac{\partial \boldsymbol{f}}{\partial \boldsymbol{x}}\right|_{\hat{\boldsymbol{x}}} =$$

$$= \begin{bmatrix} -\frac{R_1 + R_n}{L_1} & 0 & \frac{R_1 + R_n}{L_1} & (R_1 + R_n) \\ 0 & -\frac{R'_2 + R'_l}{L'_2} & \frac{R'_2 + R'_l}{L'_2} & 0 \\ \frac{R_c}{L_1} & \frac{R_c}{L'_2} & -R_c\left(\left(\frac{L_1 + L'_2}{L_1 L'_2}\right) + a_1 + \gamma a_\gamma \lambda_m^{\gamma-1}\right) & 0 \\ 0 & 0 & 0 & 0 \end{bmatrix} \tag{20}$$

$$\boldsymbol{N} = \left.\frac{\partial \boldsymbol{f}}{\partial \boldsymbol{\omega}}\right|_{\hat{\boldsymbol{x}}} = \boldsymbol{I}^{4\times 4} \tag{21}$$

$$\boldsymbol{C} = \left.\frac{\partial \boldsymbol{h}}{\partial \boldsymbol{x}}\right|_{\hat{\boldsymbol{x}}} = \begin{bmatrix}\frac{1}{L_1} & \frac{1}{L'_2} & -\left(\frac{L_1 + L'_2}{L_1 L'_2}\right) & -1\end{bmatrix} \tag{22}$$

$$\boldsymbol{M} = \left.\frac{\partial \boldsymbol{h}}{\partial \boldsymbol{v}}\right|_{\hat{\boldsymbol{x}}} = 1 \tag{23}$$

IV. Implementation and Discussion

The feasibility and accuracy of the proposed EKF-based method are verified using experimental data acquired from a laboratory test setup, numerous simulations considering different power system operating conditions, and the historical GMD event of March 1989. The proposed EKF-based estimator is implemented using the transformer differential current, measured by CTs. The GIC impact on CT saturation is minor, laying no effects on measurements [29].

0278-0046 (c) 2021 IEEE. Personal use is permitted, but republication/redistribution requires IEEE permission. See http://www.ieee.org/publications_standards/publications/rights/index.html for more information.
Authorized licensed use limited to: b-on: UNIVERSIDADE DO PORTO. Downloaded on July 08,2021 at 16:36:40 UTC from IEEE Xplore. Restrictions apply.

This article has been accepted for publication in a future issue of this journal, but has not been fully edited. Content may change prior to final publication. Citation information: DOI 10.1109/TIE.2021.3094488, IEEE Transactions on Industrial Electronics

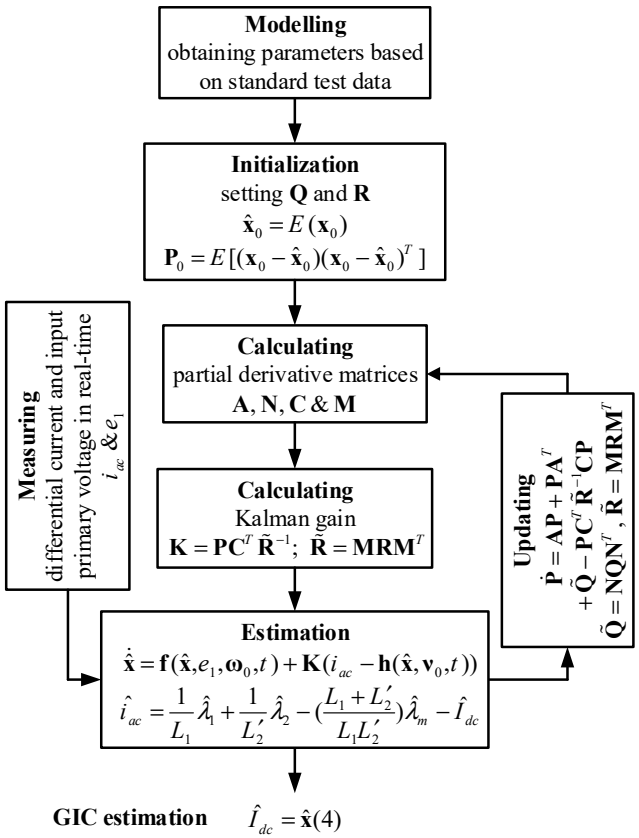

Fig. 3. Estimation process of the proposed approach.

The proposed estimator employs a sample rate of 10 samples per cycle. Conventional digital differential relays commonly utilize a sampling rate within a range of 12 to 96 samples per cycle [30]. Nevertheless, the rather low sampling resolution of 10 samples per cycle has been adopted to demonstrate the adaptability and the strength of the proposed approach. It is worth noting that the variation rate of GICs, being within the frequency range of one to a several mHz [1], is in the order of tens of seconds, which is very low with respect to the one-tenth-of-a-cycle sampling interval used for the EKF algorithm implemented. Therefore, to consider GICs as DCs, and to accordingly assume their variation rate to be equal to zero, as in equation (16), is justified and does not affect the generality of the proposed method.

It is useful to note that the proposed EKF-based GIC estimator is constructed on a physical basis, and as such makes use of the transformer parameters that are normally provided by the manufacturer. Even though the manufacturer data might be unavailable in some cases, the proposed GIC estimator can still use computed transformer data.

The well-known *short-circuit* and *open-circuit* tests are widely accepted techniques to calculate the transformer's winding resistances and leakage inductances, core loss equivalent resistance, and magnetizing characteristic's linear part. In order to compute the transformer's magnetizing characteristic beyond the knee point, various approaches can be applied, e.g., extending the *open-circuit* test into saturation region, using the core material's *B-H* curve, and other novel techniques [20]-[22]. Although transformer parameter estimation is beyond the scope of this study, yet a simple technique to calculate the transformer's saturation characteristic is briefed for the experimental GIC estimation laboratory test setup.

The performance of the proposed EKF-based estimator is evaluated using the indexes in (24)-(27):

$$[Abs.\ Error]_j = \left|I_{dc}(j) - \hat{I}_{dc}(j)\right|;\ j = 1,2,3,\dots,n\ , \quad (24)$$

$$Avg.Error = \frac{\sum_{j=1}^{n}[Abs.\ Error]_j}{n};\ j = 1,2,3,\dots,n\ , \quad (25)$$

$$[Error\%]_j = \frac{\left|I_{dc}(j) - \hat{I}_{dc}(j)\right|}{I_{dc}(j)} \times 100;\ j = 1,2,3,\dots,n\ , \quad (26)$$

$$Avg.Error\% = \frac{\sum_{j=1}^{n}[Error\%]_j}{n};\ j = 1,2,3,\dots,n\ . \quad (27)$$

In the following, performance evaluation and discussion are made regarding the results obtained from the implementation of the proposed approach, using the abovementioned indexes.

A. Experimental implementation

1) *Test Setup Description*

The test circuit, as shown in Fig. 4, has been established in resemblance to the simplest GIC loop consisting of two transformers and an electrical link in between. Transformers T_1 and T_2 are two identical single-phase transformers with the rated power of 600 VA, and the voltage ratio of 110/110 V, also utilized in [5]. T_2 is selected as the transformer of interest.

A battery unit serving as a DC voltage source is inserted to represent the effect of GICs. To prevent unwanted transients, the circuit is first energized with S_1 closed and S_2 open, and then the DC source is applied by closing S_2 and opening S_1 in the given order. It should be mentioned that for the sake of topology preservation, the bypass resistor, R_b, used to prevent short-circuit of the DC source during the time both S_1 and S_2 are closed, is selected equal to the battery unit internal resistance.

As depicted in Fig. 4, a Tektronix TDS2024C digital oscilloscope is used to ascertain the primary voltage and the differential current of T_2 from a resistive voltage divider and two CTs, respectively.

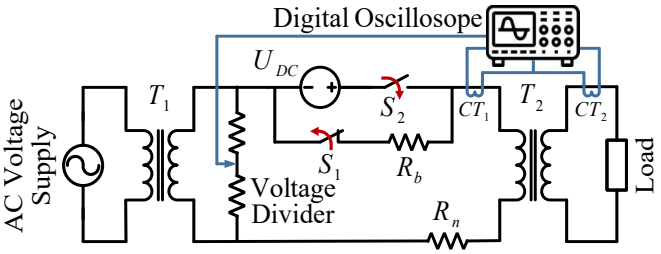

Fig. 4. The established experimental test setup.

The model parameters required by the EKF algorithm have been derived via tests conducted on the transformer of interest. Along with *short-circuit* and *open-circuit* tests, the RMS *V-I* characteristic of T_2 has been measured and then converted into peak instantaneous characteristic λ_m-i_m via "*L nonlinear data function*" element in EMTP-RV [31].

Thereafter, an odd-order polynomial in the form of equation (3) is fitted to the derived saturation characteristic, employing the Levenberg-Marquardt algorithm. The obtained model parameters are tabulated in Table I.

0278-0046 (c) 2021 IEEE. Personal use is permitted, but republication/redistribution requires IEEE permission. See http://www.ieee.org/publications_standards/publications/rights/index.html for more information.
Authorized licensed use limited to: b-on: UNIVERSIDADE DO PORTO. Downloaded on July 08,2021 at 16:36:40 UTC from IEEE Xplore. Restrictions apply.

This article has been accepted for publication in a future issue of this journal, but has not been fully edited. Content may change prior to final publication. Citation information: DOI 10.1109/TIE.2021.3094488, IEEE Transactions on Industrial Electronics

Moreover, the accuracies of the measurements and the process are reflected by matrices $\boldsymbol{R}$ and $\boldsymbol{Q}$, acquired via the approach described in *Section II*, given by:

$\boldsymbol{R} = 0.1$, $\boldsymbol{Q}$ = diag([*0.2, 0.2, 0.05, 0.01*])

To begin with the evaluation, the performance of the proposed estimation technique has been tested considering four different cases; taking the condition with the input voltage of one per-unit (p.u.) for the transformer under 50% loading and having the DC voltage source U_{dc} set to drive a DC current, I_{dc} equal to 0.15 p.u. as the base case, and varying the three involving parameters of input voltage, loading, and I_{dc} for analyzing their effect, respectively.

It is worth mentioning that the rated crest current of the transformer of interest, in this paper, is selected as the per-unit base for quantification of the driven I_{dc}. In addition, with the resolution of the employed digital oscilloscope being 2500 samples per record, the adopted sampling rate of 10 samples per cycle is attained by the time scale of 500 ms/div.

Fig. 5 shows the samples of differential current used in the proposed estimator for the observed cases described above.

The DC component of the neutral current, indicated through the multiplication of the voltage across the neutral resistor, R_n, by its resistance, is adopted as a measure of the true value of the flowing DC current, I_{dc}. Such is obtained by applying Fourier transform to the recorded neutral current. The measured and the estimated values for I_{dc} corresponding to the above-mentioned example cases are illustrated in Fig. 6.

As shown in Fig. 6, the proposed method can accurately perform under various conditions of the system. However, taking a more precise overlook on Fig. 6, a slight mismatch is visible between the measured and estimated GIC within the half-second time interval after DC source insertion. During this time span, the variation of the DC component is rather high, violating the consideration in equation (16). Nevertheless, the proposed estimator has been able to deal with interferences robustly, even in the face of model violation as noted.

In favor of a thorough evaluation, 36 experiments have been carried out considering various operating conditions of the test case under different GIC levels.

The performance of the proposed EKF-based approach has been analyzed in comparison with the methods presented in [13] and [16], referred to as *R.P.* and *2nd H.*, in terms of estimation error. The experimental test results are analyzed in the following.

2) *Different Transformer Loadings*

Considering three conditions of no-load, half-load, and full-load, under one p.u. excitation voltage, the experimental setup is subjected to six GIC levels of 0.05, 0.1, 0.15, 0.2, 0.25, and 0.3 p.u., forming a total of 18 cases to investigate.

TABLE I
SPECIFICATIONS FOR THE EXPERIMENTAL CIRCUIT

Parameter	R_1	L_1	R'_2	L'_2	R_c	R_n	a_1	a_γ	γ
Value	0.242 [Ω]	4.044 [mH]	0.262 [Ω]	6.108 [mH]	12 [kΩ]	1 [Ω]	0.9847	84.04	7

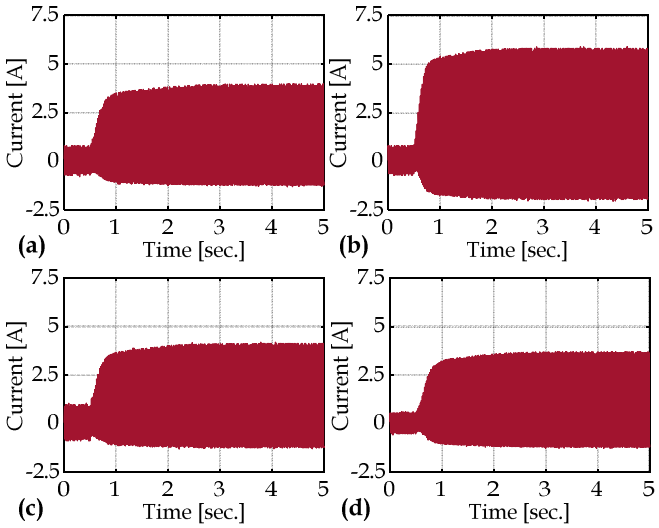

Fig. 5. Samples of differential current used in the proposed estimator: (a) 1 p.u. input voltage, 50% loading, 0.15 p.u. GIC; (b) 1 p.u. input voltage, 50% loading, 0.25 p.u. GIC; (c) 1.05 p.u. input voltage, 50% loading, 0.15 p.u. GIC; (d) 1 p.u. input voltage, 100% loading, 0.15 p.u. GIC.

The required signals are recorded and fed to the algorithms of *R.P.*, *2nd H.*, and the proposed EKF-based methods. Fig. 7 represents the estimation errors corresponding to each method, given the loading and GIC level considered.

It is well observed that although the methods of *R.P.* and *2nd H.* fail to accurately estimate the flowing GICs upon the increase in load and GIC level, the EKF-based method preserves its accuracy in estimating I_{dc} with the highest precision.

3) *Different Excitation Voltages*

With the transformer loading of 75%, three excitation levels of 0.95, 1.00, and 1.05 per-unit are considered. Six GIC levels of 0.05, 0.1, 0.15, 0.2, 0.25, and 0.3 p.u. are applied to the test transformer, forming a total of 18 cases. Likewise, the required signals are recorded and fed to the *R.P.*, *2nd H.*, and EKF estimators. The estimation errors corresponding to each estimator, given the considered excitation and GIC conditions, are depicted in Fig. 8. It is observable that the proposed EKF-based estimator provides the best performance in GIC estimation with the highest accuracy comparing to the *R.P.* and *2nd H.* methods.

4) *Implementation Results*

The performance of the proposed estimator was put into evaluation under different operation conditions. To sum up, an overall comparison between the proposed and the previous methods can be introduced by the maximum *Error%*, and the *Avg. Error%* among the total number of cases (n=36), from equations (26) and (27). The maximum and the average error percentages of each of the estimators are given in Table II.

The superiority of the proposed approach over the existing methods is distinctly highlighted in Table II. Such promising performance is achieved considering the inherent capability of the EKF to deal with the nonlinear complexities introduced via GIC flow. Present methods, assuming quasi-linear behaviors by GIC levels, fail to accurately estimate GICs under various operation conditions. Contrarily, EKF performs an indirect estimation based on the available measurements provided.

0278-0046 (c) 2021 IEEE. Personal use is permitted, but republication/redistribution requires IEEE permission. See http://www.ieee.org/publications_standards/publications/rights/index.html for more information.
Authorized licensed use limited to: b-on: UNIVERSIDADE DO PORTO. Downloaded on July 08,2021 at 16:36:40 UTC from IEEE Xplore. Restrictions apply.

This article has been accepted for publication in a future issue of this journal, but has not been fully edited. Content may change prior to final publication. Citation information: DOI 10.1109/TIE.2021.3094488, IEEE Transactions on Industrial Electronics

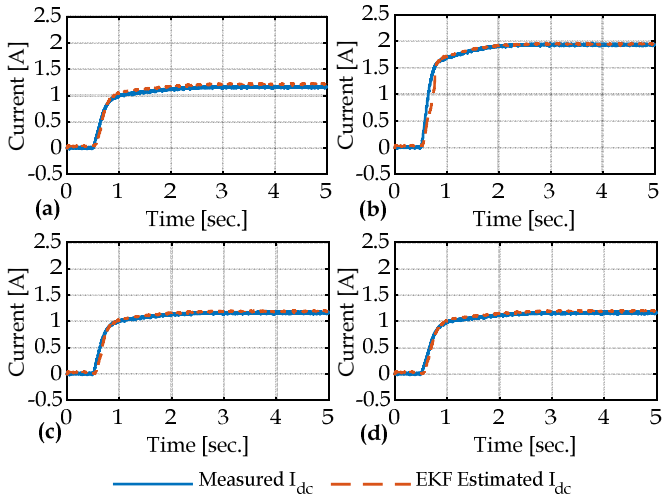

Fig. 6. Experimental implementation results of the proposed method: (a) 1 p.u. input voltage, 50% loading, 0.15 p.u. GIC (3.54% error); (b) 1 p.u. input voltage, 50% loading, 0.25 p.u. GIC (2.86% error); (c) 1.05 p.u. input voltage, 50% loading, 0.15 p.u. GIC (2.81% error); (d) 1 p.u. input voltage, 100% loading, 0.15 p.u. GIC (1.85% error).

TABLE II
COMPARISON BETWEEN THE PROPOSED AND THE PREVIOUS METHODS

Method	Ref.	Max. Error%	Avg. Error%
R.P.	[13]	74.24%	27.77%
2nd H.	[16]	19.98%	9.10%
EKF	Proposed	4.90%	3.25%

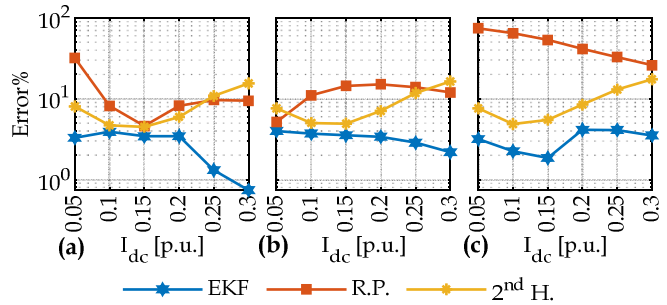

Fig. 7. GIC estimation error under different loadings: (a) No-load; (b) Half-load; (c) Full-load.

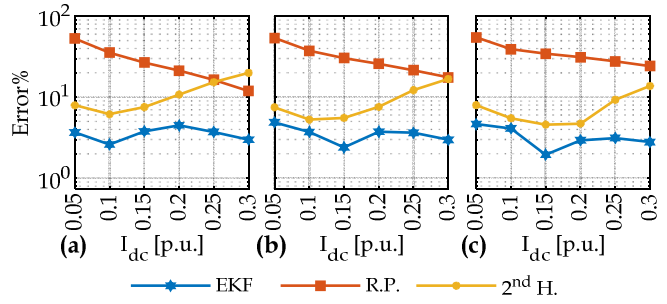

Fig. 8. GIC estimation error under different excitation voltages: (a) 0.95 p.u. (b) 1.00 p.u. (c) 1.05 p.u.

B. GMD event of March 1989

The proposed method's feasibility was put forward through experimental implementation on a single-phase laboratory test setup. However, the capability of the proposed approach is to be evaluated on a real power system scale. Nevertheless, as the required measurements during a real GMD case are not publicly available, the proposed estimator is implemented on the modified IEEE-39 benchmark system for GMD studies [32], provided in the EMTP-RV software environment.

1) *Specifications for the EKF-based Estimator*

Out of consideration for traceability and future reference, the *Load08* transformer is selected to implement the proposed estimator. The chosen transformer is a three-phase transformer, with the parameters given in Table III, and the magnetizing characteristic according to field tests on a single-phase shell-form 300MVA 765kV/120kV transformer [33].

Likewise, the measurements and the process accuracy are reflected by matrices $\boldsymbol{R}$ and $\boldsymbol{Q}$, obtained through the technique explained in Section II, given as:

$\boldsymbol{R} = 0.2$, $\boldsymbol{Q}$ = diag([*0.4, 0.4, 0.07, 0.02*])

TABLE III
THE SPECIFICATIONS FOR THE *LOAD08* TRANSFORMER

Parameter	Value	
Rated Power	700	[MVA]
Rated Frequency	60	[Hz]
Ratio	345/25/15	[kV]
Primary Winding Resistance	0.654	[Ω]
Secondary Winding Resistance	0.009	[mΩ]
Tertiary Winding Resistance	1.919	[mΩ]
Primary Winding Inductance	41.72	[mH]
Secondary Winding Inductance	0.0011	[mH]
Tertiary Winding Inductance	0.2545	[mH]
Core Loss Resistance	85.018	[kΩ]
Per-Unit Magnetizing Characteristic	$11.31\times10^{-3}\lambda_m+5.083\times10^{-3}\lambda_m^{11}$	

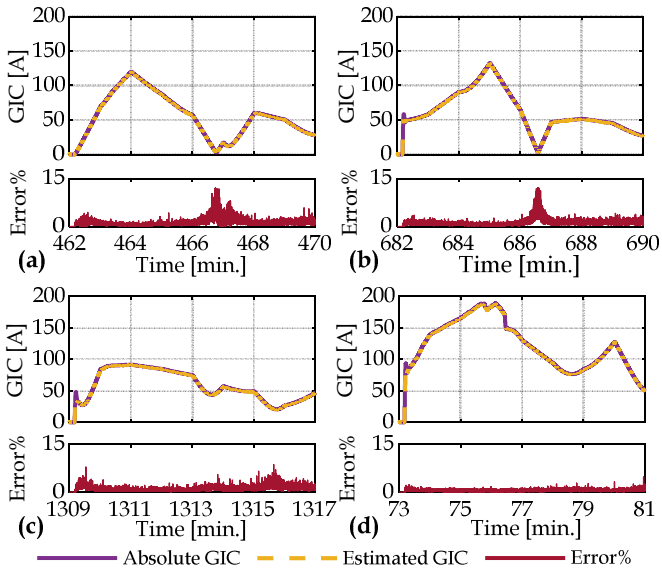

Fig. 9. Estimation results from the GMD event of 1989: (a) March 13, 07:42-08:00; (b) March 13, 11:22-11:30; (c) March 13, 21:49-21:57; (d) March 14, 01:13-01:21.

2) *Implementation Results*

The adopted benchmark is subjected to the GEF, estimated based on the earth conductivity model near Ottawa city, Canada, during the GMD event of March 13 and 14, 1989, as reported in [12].

The evaluation of the proposed method is carried out via the GMD scenarios in [32], characterizing four 8-minute excerpts from the reported data. The obtained single-phase differential current of the transformer is fed to the EKF-based estimator at

0278-0046 (c) 2021 IEEE. Personal use is permitted, but republication/redistribution requires IEEE permission. See http://www.ieee.org/publications_standards/publications/rights/index.html for more information.
Authorized licensed use limited to: b-on: UNIVERSIDADE DO PORTO. Downloaded on July 08,2021 at 16:36:40 UTC from IEEE Xplore. Restrictions apply.

This article has been accepted for publication in a future issue of this journal, but has not been fully edited. Content may change prior to final publication. Citation information: DOI 10.1109/TIE.2021.3094488, IEEE Transactions on Industrial Electronics

the sample rate of 10 samples per cycle, in accordance with the previously alluded discussion.

Due to flowing within all three phases, the single-phase estimated GIC is multiplied by three. As for a comparison reference, the absolute GIC flown in the transformer under study is characterized by the DC component of the transformer neutral current. The results from the simulation of the scenarios are depicted in Fig. 9 and summarized in Table IV.

From Fig. 9 and Table IV, it is evident that the proposed approach can successfully estimate GIC flow in a realistic power system with high accuracy. It should be mentioned that the proposed method estimates GICs by a reasonably low absolute error; the error percentage is increased under low GICs, due to the division of absolute errors by small values.

TABLE IV
PERFORMANCE OF THE PROPOSED METHOD FOR THE 1989 GMD EVENT

Scn.	Date	Time (UTC)	Max. Abs. Error [A]	Avg. Error [A]	Max. Error%	Avg. Error%
1	3/13/1989	07:42-08:00	3.285	0.466	11.98	1.156
2	3/13/1989	11:22-11:30	3.166	0.505	11.99	1.072
3	3/13/1989	21:49-21:57	3.320	0.521	8.640	1.060
4	3/14/1989	01:13-01:23	4.172	0.621	4.709	0.543

3) *Performance Comparison with GIC Simulation Techniques*

The robustness of the proposed estimator's performance over the methods presented in [13] and [16] was ensured based on the experimental studies conducted in the previous sub-sections. There are other comprehensive ways of GIC estimation that are developed based on power system simulation, using geomagnetic field measurements obtained from geomagnetism observatory stations. These methods make use of the Earth's conductivity to calculate the induced GEFs, based on the data which are obtained from geomagnetism observatories. The GICs are then computed by solving a network's model using the calculated GEF-resultant DC potentials along transmission lines. In these methods, the simplifying assumptions and approximations associated with each computation step add a level of error, which altogether, leads to more inaccurate results.

Primarily, the magnetic field data are not ideally available in the vicinity of the power network circuits. In fact, the geomagnetism observatories are positioned sparsely with large distances from each other, and thus the distribution of the geomagnetic field in the network's area should be approximated. Moreover, the field measurements may also include noise. Even though by using the technique proposed in [34], the noise effect in the magnetic field data can be reduced, the issue of lacking the exact geomagnetic field in the network's area still persists. Besides, only an approximated model can be considered for the Earth's geophysical structure and its conductivity. On the other hand, the transmission line route directions, which are important, are approximated by assuming the lines as straight paths between two substations.

Contrary to such methods which rely on non-power-system-based quantities, the proposed EKF-based estimator operates solely based on quantities inherent to power networks. These quantities are the transformer differential current which is obtained by the already available differential protection scheme, and the transformer model. Therefore, it is safe to say that the proposed EKF-based approach is robust to inaccuracies resulting from cumulative simplifying approximations in GIC simulation methods such as the one presented in [11]. Yet, a quantitative comparison between the performances of these methods and the proposed EKF-based estimator is needed.

TABLE V
CONSIDERED UNCERTAINTIES ASSOCIATED WITH GIC SIMULATION

Source of Uncertainty	Case #1	Case #2	Case #3
Geomagnetic Field Data	[13]10%	5%	0%
Line Route Paths	[16]10%	5%	0%
Earth Conductivity Structure	20%	10%	5%

Therefore, the IEEE 39 bus GMD benchmark network [32] is applied, which makes use of the transformer of *Load08* as a study reference. The comparative analysis is performed by applying the method published in [11]. The GMD scenarios introduced in Table IV are selected as the comparison basis. In order to reflect the uncertainties associated with the GIC simulation methods, corresponding to each of the scenarios in Table IV, three cases have been established considering the uncertainties according to Table V. Moreover, an amount of white Gaussian noise with a signal-to-noise ratio (SNR) of 30 dB is considered in the EKF-based estimator's input for all the cases studied. Fig. 10 shows the performances of the GIC simulation technique and the proposed approach regarding each of the cases in Table V, in terms of maximum *Abs. Error*, calculated with respect to their corresponding GMD scenario.

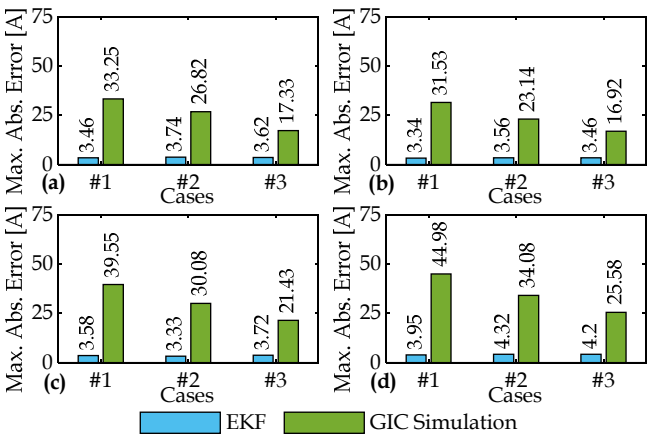

Fig. 10. Comparison between the performances of the proposed approach and the method in [11] by Max. *Abs. Error* corresponding to the cases introduced in Table V for GMD scenarios of 1989 event given in Table IV: (a) Scn. 1; (b) Scn. 2; (c) Scn. 3; (d) Scn. 4.

Fig. 10 shows the performance of the proposed EKF-based estimator. A noteworthy result achieved in this analysis is that the GIC simulation method [11] is still highly erroneous in case #3 of Table V. This case is an optimistic resemblance to the real-world case where the exact modeling of the Earth's conductivity is not possible, and therefore, it only considers a fairly low uncertainty of the Earth's conductivity structure.

C. *Effect of External Interferences*

In order to evaluate the performance of the proposed EKF-based GIC estimator under real-life interferences from the power system's operation, the modified IEEE-39 benchmark system for GMD studies [32] has been considered under

0278-0046 (c) 2021 IEEE. Personal use is permitted, but republication/redistribution requires IEEE permission. See http://www.ieee.org/publications_standards/publications/rights/index.html for more information.
Authorized licensed use limited to: b-on: UNIVERSIDADE DO PORTO. Downloaded on July 08,2021 at 16:36:40 UTC from IEEE Xplore. Restrictions apply.

This article has been accepted for publication in a future issue of this journal, but has not been fully edited. Content may change prior to final publication. Citation information: DOI 10.1109/TIE.2021.3094488, IEEE Transactions on Industrial Electronics

normal operating condition, excitation harmonic distortions, harmonics from nonlinear loads, and both excitation and nonlinear load harmonics.

To such an aim, 10000 scenarios have been simulated corresponding to each operating condition, associated with the parameters specified in Table VI being uniformly distributed within the designated ranges. Each scenario is simulated by a total run-time of 20 seconds for the system to reach a steady state. The applied GEFs gradually increase from zero to their final value within a 5-second-duration, starting at 5 sec.

The EKF estimator is implemented on *Load08*, *Load04*, *PowerPlant06*, and *PowerPlant04* transformers of the benchmark system under study. Fig. 11 shows the cumulative density of *Max. Error%* of estimation for the transformers of interest, within the scenarios studied under each operating condition of the test system.

As shown in Fig. 11, the proposed EKF-based estimator can accurately estimate the GICs flowing through transformers even under heavy external interferences, such as harmonic excitations and loadings. According to Fig. 11d, in all the studied transformers, the maximum error percentage for more than 90% of the scenarios under the worst interference condition of both harmonic loading and excitation is limited to 10%, ensuring the robustness of the proposed approach.

D. Field validation with inrush current phenomenon

Even though field data from GIC phenomena are rather rare and often inaccessible, a satisfactory trust margin can still be warranted in the proposed estimator through alternative exercises. In the previous sub-sections, firstly, the accountability of the proposed method was analyzed on a scaled-down laboratory test setup, and thereafter on a real-scale simulated test system.

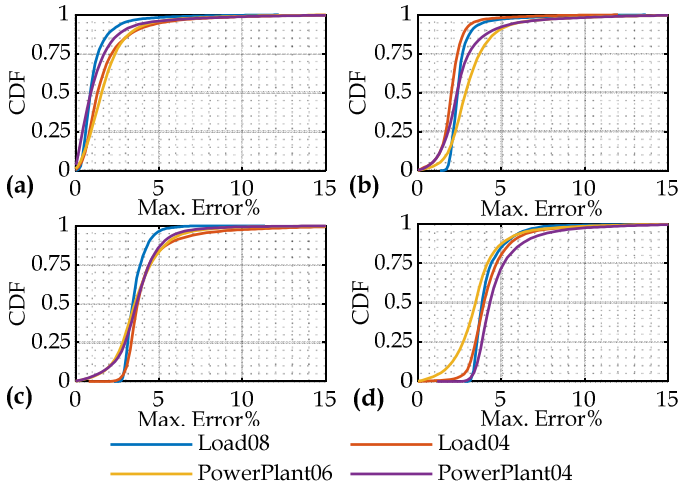

Fig. 11. The cumulative density of maximum estimation error percentage for several transformers for various operating conditions of the test system: (a) Normal condition; (b) Harmonic loading; (c) Harmonic excitation; (d) Both harmonic loading and excitation.

Further verification of the proposed EKF-based GIC estimator can be attained by transformer energization inrush current analysis, as in [16].

Even though they are essentially driven through different mechanisms, the GICs and inrush currents are both contributing to unidirectional core saturation. Moreover, the DC component of the inrush currents results in a DC voltage drop on transformer resistances, hence it can be characterized by the same estimation model as the proposed method. Therefore, the field measurements of inrush energization currents of a realistic industrial power transformer are used as a good validation reference for the proposed EKF-based GIC estimator.

TABLE VI
PERFORMANCE OF THE PROPOSED METHOD FOR THE 1989 GMD EVENT

Test Case	Excitation THD LVL. (%)	Load THD LVL. (%)	GEF [V/km]	
			E_N	E_E
Normal Condition	0	0	0-10	0-10
Harmonic Loading	0	1-20	0-10	0-10
Harmonic Excitation	0.5-10	0	0-10	0-10
Both Harmonic Loading & Excitation	0.5-10	1-20	0-10	0-10

1) *Field Testbed Transformer Specifications*

The field data have been recorded from a Yg/Δ transformer of an arc furnace used in an electro-fused magnesia industry. Due to high current ratings at the low-voltage side of an arc furnace transformer, the applied differential protection scheme is rather complex.

However, the transformer of interest is protected at its primary by an over-current and earth-fault relay and a disturbance recorder with the sampling rate of 16 samples per cycle and the per event memory of 50 cycles.

Taking into consideration that arc furnace transformers are not energized under loaded conditions, it is reasonable to adopt the inrush currents recorded at the primary of the testbed transformer upon energization equal to its differential current. Moreover, the current at the neutral point of the testbed transformer is also observed by the aforementioned protection scheme using a hall-effect sensor for harmonic monitoring purposes. The parameters of the testbed transformer are given in Table VII. The measurement and the process noise covariance matrices $\boldsymbol{R}$ and $\boldsymbol{Q}$, associated with the field testbed transformer, obtained via the technique in *Section II* are as:
$\boldsymbol{R} = 0.31$, $\boldsymbol{Q}$ = diag([$0.25, 0.25, 0.12, 0.05$])

2) *Estimation results*

The evaluation of the proposed estimator's performance has been carried out using the data from four available inrush energization incidents saved on the arc furnace transformer's disturbance recorder memory. Since the three phases draw unequal amounts of inrush currents, as for being energized on a different point on the voltage waveform, the inrush current data of the three phases are individually fed to the proposed method for each recorded incident.

Afterward, the per phase estimated DC components of each incident are summed up and then compared with their corresponding DC component of the recorded neutral current, as a reference.

The measured and estimated results from each studied inrush incident are depicted in Fig. 12. As it can be observed in Fig. 12, the proposed EKF-based estimator is swiftly able to estimate the DC component of a realistic transformer's inrush currents upon energization with high accuracy, as a phenomenon with the saturation conditions similar to the GICs. Therefore, the performance of the proposed estimator is also validated by field measurements.

0278-0046 (c) 2021 IEEE. Personal use is permitted, but republication/redistribution requires IEEE permission. See http://www.ieee.org/publications_standards/publications/rights/index.html for more information.
Authorized licensed use limited to: b-on: UNIVERSIDADE DO PORTO. Downloaded on July 08,2021 at 16:36:40 UTC from IEEE Xplore. Restrictions apply.

This article has been accepted for publication in a future issue of this journal, but has not been fully edited. Content may change prior to final publication. Citation information: DOI 10.1109/TIE.2021.3094488, IEEE Transactions on Industrial Electronics

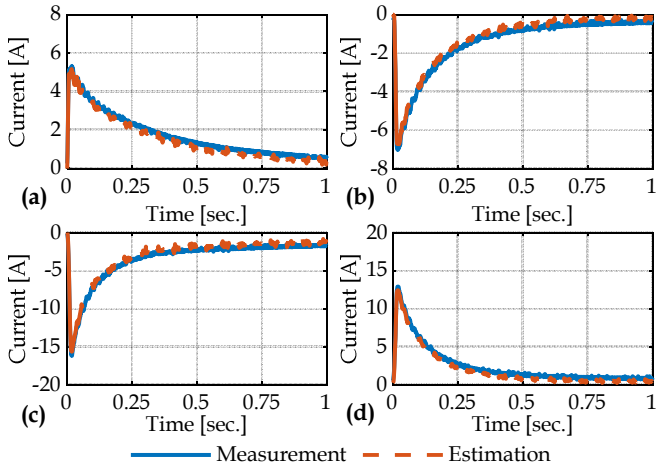

Fig. 12. Comparison between the DC component of the neutral current obtained from measurement and the of the three winding estimated DC components of the field testbed transformer: (a) *Avg. Error*=0.2055 [A]; (b) *Avg. Error*=0.23 [A]; (c) *Avg. Error*=0.4143 [A], (d) *Avg. Error*=0.45 [A].

TABLE VII
THE SPECIFICATIONS FOR THE FIELD TESTBED FURNACE TRANSFORMER

Parameter	Value	
Rated Power	2.5	[MVA]
Rated Frequency	50	[Hz]
Ratio	20/0.19	[kV]
Primary Winding Resistance	1.6133	[Ω]
Secondary Winding Resistance	0.0337	[Ω]
Primary Winding Inductance	0.1769	[mH]
Secondary Winding Inductance	0.0163	[mH]
Core Loss Resistance	38.986	[kΩ]
Per-Unit Magnetizing Characteristic	$2.04\times10^{-3}\lambda_m+8.107\times10^{-3}\lambda_m^{9}$	

E. Discussion

In order to examine the feasibility of the proposed GIC estimation method, primarily, an experimental test setup is prepared to implement the EKF-based estimator. Moreover, a comparison is made with the methods referred to as *R.P.* and *2nd H.*, corresponding to references [13] and [16], in terms of estimation error. A total of 36 cases are studied considering different operation conditions.

First, the loading effect is sought by changing the GIC flow from 0.05 p.u. to 0.3 p.u., under the input voltage of 1.00 p.u., and the transformer loadings of 0%, 50%, and 100%. Thereafter, considering the similar GIC level variation, the input voltage was set to 0.95 p.u., 1.00 p.u., and 1.05 p.u. under 75% loading for the aim of analyzing the effect of the excitation voltage. The differential current is provided by two CTs and recorded at the sample rate of 10 samples per cycle. The results indicate the unconditional superiority of the proposed method over other methods.

Additionally, in order to evaluate the performance of the proposed method on a real scale, the 39-bus IEEE benchmark system for GMD studies is employed [32]. The test system is subjected to four 8-minute excerpts from the historical data of the March 1989 GMD event, considering the Earth conductivity model of the Ottawa city region, Canada [12].

A three-phase transformer is chosen, its differential current is measured on one phase at the sample rate of 10 samples per cycle, and is then fed to the EKF algorithm for the sake of GIC estimation. It is observed that the proposed EKF estimator can accurately estimate GICs given a real GMD event in power systems.

By using this test system and the four eight-minute excerpts from the 1989 GMD event, the proposed method is compared to the method presented in [11] which was selected as a representative of GIC estimation techniques. The robustness of the proposed EKF-based estimator is validated by including the effects of the uncertainties associated with these types of methods (which comprise the geomagnetic field measurements, transmission line routes, and Earth's conductivity structure). It is also shown that even WHEN the Earth model is associated with only a fairly small uncertainty, the GIC estimation methods are still highly erroneous.

Thereafter, the robustness of the proposed EKF-based estimator is analyzed against external interferences introduced by harmonic pollutions in the grid voltages and load currents. Such an end is attained by a comparison between 4 different operating conditions of the system given as the normal condition, nonlinear loading harmonics, excitation voltage harmonics, and the latter two simultaneously. Corresponding to each condition, 10000 scenarios are studied associated with various possibilities of respective parameters. The comparison is conducted over maximum GIC estimation error percentage in four selected network transformers, for each scenario.

The results showed that the proposed estimator is resistive to external interferences, robustly preserving its accuracy of estimation during various operating conditions.

Furthermore, the proposed EKF-based estimator is validated in the field by using the inrush current data from a realistic industrial arc furnace transformer. Despite the different sources of GICs and inrush currents, they are similar due to being associated with asymmetrical core saturation conditions and DC current flows. For the performance evaluation, four logged energization incidents have been selected, and their corresponding inrush current data have been used in the proposed method for each phase individually. The estimated DC components of each winding are then summed up and compared to the DC current component recorded at the neutral conductor. The accurate consistency of the estimated results with the measured inrush currents validates the proposed EKF-based GIC estimator in the field.

To sum up, whereas the previous methods are incapable of accurate GIC estimation, the proposed EKF-based estimator appropriately deals with nonlinear complexities and external interferences, providing accurate estimations of GICs flowing through transformer windings in real-time without the need to install additional devices.

V. CONCLUSION

In this paper, a novel method was introduced to estimate the GICs flowing through power transformers. Based on the derived nonlinear state-space equations of the transformer, an EKF-based estimator was developed for indirect GIC estimation from readily available AC measurements for the transformer differential current, enabling a swift GIC estimation without additional GIC monitors. Moreover, as the EKF inherently accounted for system nonlinearity, the proposed method was able to estimate wide ranges of GICs with high accuracy. The modeling parameters required by the proposed method can be acquired from standard tests, e.g., pre-commissioning testing. The proposed approach was thoroughly validated through simulation and experimental

0278-0046 (c) 2021 IEEE. Personal use is permitted, but republication/redistribution requires IEEE permission. See http://www.ieee.org/publications_standards/publications/rights/index.html for more information.
Authorized licensed use limited to: b-on: UNIVERSIDADE DO PORTO. Downloaded on July 08,2021 at 16:36:40 UTC from IEEE Xplore. Restrictions apply.

This article has been accepted for publication in a future issue of this journal, but has not been fully edited. Content may change prior to final publication. Citation information: DOI 10.1109/TIE.2021.3094488, IEEE Transactions on Industrial Electronics

tests. To such aim, at first, a prepared test setup was subjected to GICs. The comparison between the estimated GIC from the proposed method and other previous methods with direct measurements highlighted the superiority of the proposed estimator. Hereafter, an EMTP-RV simulation of an EHV power grid, subjected to the GMD event of March 1989 in Canada, was employed to evaluate the performance of the proposed method on a realistic scale. The estimation results showed high consistency with the measurements extracted from the EMTP-RV simulation. This testbed has been utilized to validate the advantage of the proposed EKF-based estimator with respect to the simulation-based GIC estimation methods. In addition, the robustness of the proposed approach against external interferences was ensured by subjecting the test system to numerous scenarios of voltage and current harmonic distortions. The presented results confirmed the high performance of the proposed EKF-based method in robust and accurate estimation of GICs in real-time. Furthermore, by using the inrush current data from an industrial arc furnace transformer, the validity of the proposed method was also proved in the field.

REFERENCES

[1] V. Albertson et al., "Geomagnetic disturbance effects on power systems," *IEEE Trans. Pow. Deliv.*, vol. 8, no. 3, pp. 1206-1216, 1993.

[2] "Effects of Geomagnetic Disturbances on the Bulk Power System," *North American Electric Reliability Corporation (NERC)*, Feb. 2012.

[3] R. Girgis and K. Vedante, "Effects of GIC on power transformers and power systems," *PES T&D 2012*, Orlando, FL, 2012, pp. 1-8.

[4] B. Bozoki et al., "The effects of GIC on protective relaying," *IEEE Trans. Pow. Deliv.*, vol. 11, no. 2, pp. 725-739, Apr. 1996.

[5] B. Behdani et al., "On the impact of geomagnetically induced currents in driving series capacitor compensated power systems to ferroresonance," in *International Journal of Electrical Power & Energy Systems*, vol. 125, Feb. 2021, doi: 10.1016/j.ijepes.2020.106424.

[6] L. Gong, Y. Fu, M. Shahidehpour, and Z. Li, "A Parallel Solution for the Resilient Operation of Power Systems in Geomagnetic Storms," *IEEE Trans. Smart Grid*, pp. 1-1, 2019, doi: 10.1109/TSG.2019.2962669.

[7] A. Rezaei-Zare et al., "Optimal Placement of GIC Blocking Devices Considering Equipment Thermal Limits and Power System Operation Constraints," *IEEE Trans. Pow. Deliv.*, vol. 33, no. 1, pp. 200-208, 2018.

[8] M. Kazerooni, H. Zhu, and T. J. Overbye, "Mitigation of Geomagnetically Induced Currents Using Corrective Line Switching," *IEEE Trans. Power Syst.*, vol. 33, no. 3, pp. 2563-2571, 2018.

[9] L. Bolduc, "GIC observations and studies in the Hydro-Québec power system," *J. Atmos. Solar-Ter. Phys.*, vol. 64, no. 16, pp. 1793-1802, 2002.

[10] T. J. Overbye et al., "Integration of geomagnetic disturbance modeling into the power flow: A methodology for large-scale system studies," *2012 North American Power Symposium (NAPS)*, Sept. 2012, pp. 1-7.

[11] L. Marti et al., "Simulation of Geomagnetically Induced Currents With Piecewise Layered-Earth Models," *IEEE Trans. Pow. Deliv.*, vol. 29, no. 4, pp. 1886-1893, Aug. 2014.

[12] L. Marti, A. Rezaei-Zare, and D. Boteler, "Calculation of Induced Electric Field During a Geomagnetic Storm Using Recursive Convolution," *IEEE Trans. Pow. Del.*, vol. 29, no. 2, pp. 802-807, 2014.

[13] L. Marti et al., "Determination of Geomagnetically Induced Current Flow in a Transformer From Reactive Power Absorption," *IEEE Trans. Pow. Deliv.*, vol. 28, no. 3, pp. 1280-1288, 2013.

[14] R. L. Lesher, J. W. Porter, and R. T. Byerly, "SUNBURST/spl minus/a network of GIC monitoring systems," *IEEE Trans. Pow. Deliv.*, vol. 9, no. 1, pp. 128-137, 1994, doi: 10.1109/61.277687.

[15] P. Ripka et al., "Measurement of DC Currents in the Power Grid by Current Transformer," *IEEE Tran. Mag.*, vol. 49, no. 1, pp. 73-76, 2013.

[16] E. E. Bernabeu, "Single-Phase Transformer Harmonics Produced During Geomagnetic Disturbances: Theory, Modeling, and Monitoring," *IEEE Trans. on Pow. Deliv.*, vol. 30, no. 3, pp. 1323-1330, 2015.

[17] R. A. Walling, "Potential impacts of harmonics on bulk system integrity during geomagnetic disturbances," *2013 IEEE Power & Energy Society General Meeting*, Vancouver, BC, 2013, pp. 1-5.

[18] J. Chen et al., "Power system responses to geomagnetic disturbances recognized using phasor measurement recordings," *Int. J. Electr. Power Energy Syst.*, vol. 113, pp. 932-940, Dec. 2019.

[19] S. Wang, P. Dehghanian, L. Li, and B. Wang, "A Machine Learning Approach to Detection of Geomagnetically Induced Currents in Power Grids," *IEEE Trans. Ind. Apps.*, vol. 56, no. 2, pp. 1098-1106, 2020.

[20] S. G. Abdulsalam, X. Wilsun, W. L. A. Neves, and L. Xian, "Estimation of transformer saturation characteristics from inrush current waveforms," *IEEE Trans. Pow. Deliv.*, vol. 21, no. 1, pp. 170-177, 2006.

[21] T. C. Monteiro et al., "Transformer Operation at Deep Saturation: Model and Parameter Determination," *IEEE Trans. Ind. App.*, vol. 48, no. 3, pp. 1054-1063, Jun. 2012, doi: 10.1109/TIA.2012.2190256.

[22] Q. Wu, T. Hong, S. Jazebi, and F. d. León, "Experimentally Validated Method to Measure the λ-i Characteristics of Asymmetric Three-Phase Transformers," *IEEE Trans. Magnetics*, vol. 55, no. 4, pp. 1-9, 2019.

[23] D. H. Boteler and R. J. Pirjola, "Modelling geomagnetically induced currents produced by realistic and uniform electric fields," *IEEE Trans. Pow. Deliv.*, vol. 13, no. 4, pp. 1303-1308, 1998.

[24] J. A. Martinez and B. A. Mork, "Transformer modeling for low- and mid-frequency transients - a review," *IEEE Trans. Pow. Deliv.*, vol. 20, no. 2, pp. 1625-1632, 2005.

[25] D. Simon, *Optimal State Estimation: Kalman, H Infinity, and Nonlinear Approaches.* Wiley, 2006.

[26] F. Naseri et al., "Fast Discrimination of Transformer Magnetizing Current From Internal Faults: An Extended Kalman Filter-Based Approach," *IEEE Trans. Pow. Deliv.*, vol. 33, no. 1, pp. 110-118, 2018.

[27] S. Sharifinia et al., "Extended Kalman Filter-Based Approach for Nodal Pricing in Active Distribution Networks," *IEEE Syst. Journal*, doi: 10.1109/JSYST.2020.2986686.

[28] G. Rigatos, P. Siano, and N. Zervos, "Sensorless Control of Distributed Power Generators With the Derivative-Free Nonlinear Kalman Filter," *IEEE Trans. Ind. Electron.*, vol. 61, no. 11, pp. 6369-6382, 2014.

[29] Y. Zhao and P. Crossley, "Impact of DC bias on differential protection of converter transformers," *Int. J. of Electr. Power Energy Syst.*, vol. 115, p. 105426, Feb. 2020.

[30] Phadke, Arun G., and James S. Thorp. *Computer Relaying for Power Systems.* John Wiley & Sons, 2009.

[31] H. W. Dommel, *EMTP Theory Book*, Microtran Power System Analysis Corporation, Vancouver, British Columbia, May, 1992.

[32] Luc Gerin-Lajoie et al., "Simultaneous DC and AC Simulation of GMD Impacts in a Power System," *International Conference on Power Systems Transients (IPST)*, Perpignan, France, 2019.

[33] C. Morin and B. Khodabakhchian, "765kV power transformer losses upon energizations: A comparison between field test measurements and EMTP-RV simulations," *Elec. Pow. Sys. Res.*, vol. 115, pp. 35-42, 2014.

[34] M. Ariannik et al., "Processing Magnetometer Signals for Accurate Wide-Area Geomagnetic Disturbance Monitoring and Resilience Analysis," *IEEE Trans. Pow. Del.*, doi: 10.1109/TPWRD.2020.3024908.

Behzad Behdani received the B.Sc. degree in Electrical Power Engineering from the University of Birjand, Birjand, Iran, in 2017, and the M.Sc. degree in Electrical Power Systems Engineering from the Shiraz University, Shiraz, Iran, in 2020. His research interests include transients in electrical systems, power system protection, and geomagnetically induced currents in power systems.

Mohsen Tajdinian received the B.Sc. degree from the Jundi-Shapur University of Technology, Dezful, Iran, in 2012, the M.Sc. degree from the Amirkabir University of Technology, Tehran, Iran, in 2015, and the Ph.D. degree from the Shiraz University, Shiraz, Iran, in 2020, all in electrical engineering. His research interests include power system stability and power system protection.

0278-0046 (c) 2021 IEEE. Personal use is permitted, but republication/redistribution requires IEEE permission. See http://www.ieee.org/publications_standards/publications/rights/index.html for more information.
Authorized licensed use limited to: b-on: UNIVERSIDADE DO PORTO. Downloaded on July 08,2021 at 16:36:40 UTC from IEEE Xplore. Restrictions apply.

This article has been accepted for publication in a future issue of this journal, but has not been fully edited. Content may change prior to final publication. Citation information: DOI 10.1109/TIE.2021.3094488, IEEE Transactions on Industrial Electronics

Mehdi Allahbakhshi received the B.Sc. degree from the Khajeh Nasir Toosi University of Technology, Tehran, Iran, in 1999, the M.Sc. degree from the Sharif University of Technology, Tehran, Iran, in 2001, and the Ph.D. degree from the Khajeh Nasir Toosi University of Technology, Tehran, Iran, in 2011, all in Electrical Power Engineering. He is currently an Associate Professor with the School of Electrical and Computer Engineering, Shiraz University, Shiraz, Iran. His research interests include high-voltage engineering, insulation systems and transients in electrical systems.

Marjan Popov (Senior Member, IEEE) obtained his Ph.D. degree in electrical power engineering from Delft University of Technology, Delft, The Netherlands, in 2002. He is also a Chevening Alumnus and, in 1997, he was an Academic Visitor with the University of Liverpool, Liverpool, U.K., working in the Arc Research Group on modeling SF6 circuit breakers. His major fields of interest are in future power systems, large-scale power system transients, intelligent protection for future power systems, and wide-area monitoring and protection. He is a member of Cigre and actively participated in WG C4.502 and WG A2/C4.39. In 2010, he received the prestigious Dutch Hidde Nijland Prize for extraordinary research achievements. He was the recipient of the IEEE PES Prize Paper Award and IEEE Switchgear Committee Award in 2011 and an Associate Editor for Elsevier's International Journal of Electrical Power and Energy Systems. In 2017, together with the Dutch utilities TenneT, Alliander and Stedin he founded the Dutch Power System Protection Centre to promote the research and education in power system protection.

Miadreza Shafie-khah (Senior Member, IEEE) received the Ph.D. degree in electrical engineering from Tarbiat Modares University, Tehran, Iran, and the Ph.D. degree in electromechanical engineering from the University of Beira Interior (UBI), Covilha, Portugal. He held a postdoctoral position with UBI and the University of Salerno, Salerno, Italy. He is currently an Associate Professor at the University of Vaasa, Vaasa, Finland. He has coauthored more than 368 articles that received more than 6500 citations with an H-index = 46. His research interests include power market simulation, market power monitoring, power system optimization, demand response, electric vehicles, price and renewable forecasting, and smart grids. He is a Top Scientist in the Guide2Research Ranking in computer science and electronics. He has won five best paper awards at IEEE conferences. He was considered one of the outstanding reviewers of the IEEE TRANSACTIONS ON SUSTAINABLE ENERGY, in 2014 and 2017; one of the best reviewers of the IEEE TRANSACTIONS ON SMART GRID, in 2016 and 2017; one of the outstanding reviewers of the IEEE TRANSACTIONS ON POWER SYSTEMS, in 2017 and 2018; and one of the outstanding reviewers of IEEE OPEN ACCESS JOURNAL OF POWER AND ENERGY (OAJPE), in 2020. He is an Editor of the IEEE TRANSACTIONS ON SUSTAINABLE ENERGY, an Associate Editor of the IEEE SYSTEMS JOURNAL, an Editor of IEEE OAJPE, an Associate Editor of IET-RPG, the Guest Editor-in-Chief of IEEE OAJPE, and a Guest Editor of IEEE TRANSACTIONS ON CLOUD COMPUTING and more than 14 special issues. He is also a Volume Editor of the book Blockchain-Based Smart Grids (Elsevier, 2020).

João P. S. Catalão (Senior Member, IEEE) received the M.Sc. degree from the Instituto Superior Técnico (IST), Lisbon, Portugal, in 2003, and the Ph.D. degree and Habilitation for Full Professor ("Agregação") from the University of Beira Interior (UBI), Covilha, Portugal, in 2007 and 2013, respectively.

Currently, he is a Professor at the Faculty of Engineering of the University of Porto (FEUP), Porto, Portugal, and Research Coordinator at INESC TEC. He was also appointed as Visiting Professor by North China Electric Power University (NCEPU), Beijing, China. He was the Primary Coordinator of the EU-funded FP7 project SiNGULAR ("Smart and Sustainable Insular Electricity Grids Under Large-Scale Renewable Integration"), a 5.2-million-euro project involving 11 industry partners. He has authored or coauthored more than 885 publications, including 425 international journal papers (130 IEEE Transactions/Journal papers), 415 international conference proceedings papers (vast majority co-sponsored by IEEE), 4 books and 41 book chapters, with an *h*-index of 68, an *i10*-index of 335, and over 18,300 citations (according to Google Scholar), having supervised more than 85 post-docs, Ph.D. and M.Sc. students. He was the General Chair of SEST 2019, technically sponsored by IEEE PES and IEEE IES, the General Co-Chair of SEST 2020, technically sponsored by IEEE PES, IEEE IES and IEEE IAS, and also the Honorary Chair of SEST 2021, technically sponsored by IEEE PES, IEEE IES, IEEE IAS and IEEE PELS. He is the Editor of the books entitled *"Electric Power Systems: Advanced Forecasting Techniques and Optimal Generation Scheduling"* and *"Smart and Sustainable Power Systems: Operations, Planning and Economics of Insular Electricity Grids"* (Boca Raton, FL, USA: CRC Press, 2012 and 2015, respectively). His research interests include power system operations and planning, distributed renewable generation, power system economics and electricity markets, demand response and smart grid.

Prof. Catalão is the Senior Editor of the IEEE TRANSACTIONS ON SMART GRID, the Promotion and Outreach (Senior) Editor of the IEEE OPEN ACCESS JOURNAL OF POWER AND ENERGY, an Associate Editor of the IEEE TRANSACTIONS ON POWER SYSTEMS, an Associate Editor of the IEEE POWER ENGINEERING LETTERS, an Associate Editor of the IEEE TRANSACTIONS ON INDUSTRIAL INFORMATICS, an Associate Editor of the IEEE TRANSACTIONS ON NEURAL NETWORKS AND LEARNING SYSTEMS, an Associate Editor of the IEEE TRANSACTIONS ON INTELLIGENT TRANSPORTATION SYSTEMS, an Associate Editor of the IEEE TRANSACTIONS ON CLOUD COMPUTING, an Associate Editor of the IEEE TRANSACTIONS ON INDUSTRY APPLICATIONS, an Associate Editor of the IEEE SYSTEMS JOURNAL, and an Associate Editor of IEEE ACCESS. From 2011 till 2018 he was an Associate Editor of the IEEE TRANSACTIONS ON SUSTAINABLE ENERGY, and from 2013 till 2020 he was an Associate Editor of the IEEE TRANSACTIONS ON SMART GRID. He was the *Guest Editor-in-Chief* for the Special Section on "Real-Time Demand Response" of the IEEE TRANSACTIONS ON SMART GRID, published in December 2012, the *Guest Editor-in-Chief* for the Special Section on "Reserve and Flexibility for Handling Variability and Uncertainty of Renewable Generation" of the IEEE TRANSACTIONS ON SUSTAINABLE ENERGY, published in April 2016, and the *Corresponding/Lead Guest Editor* (*Guest Editor-in-Chief*) for the Special Section on "Industrial and Commercial Demand Response" of the IEEE TRANSACTIONS ON INDUSTRIAL INFORMATICS, published in November 2018. Currently, he is the *Guest Editor-in-Chief* for the Special Section on "Demand Response Applications of Cloud Computing Technologies" of the IEEE TRANSACTIONS ON CLOUD COMPUTING, and also the *Guest Lead Editor* (*Guest Editor-in-Chief*) for the Special Section on "Real-World Challenges of TSO-DSO Coordination" of the IEEE TRANSACTIONS ON POWER SYSTEMS. He was the recipient of the 2011 Scientific Merit Award UBI-FE/Santander Universities, the 2012 Scientific Award UTL/Santander Totta, the 2016-2019 (four years in a row) FEUP Diplomas of Scientific Recognition, the 2017 Best INESC-ID Researcher Award, and the 2018 Scientific Award ULisboa/Santander Universities. He is a *Top Scientist* in the Guide2Research Ranking (number one in Portugal), which lists only scientists having *h*-index equal or greater than 40. Moreover, he has won 5 *Best Paper Awards* at IEEE Conferences.

0278-0046 (c) 2021 IEEE. Personal use is permitted, but republication/redistribution requires IEEE permission. See http://www.ieee.org/publications_standards/publications/rights/index.html for more information.
Authorized licensed use limited to: b-on: UNIVERSIDADE DO PORTO. Downloaded on July 08,2021 at 16:36:40 UTC from IEEE Xplore. Restrictions apply.